JOURNAL OF SPACECRAFT AND ROCKETS
Vol. 46, No. 1, January–February 2009

Assessment of Straight Tapered Geometry Approximations of Raked-Tip Wings

William B. Blake*
U.S. Air Force Research Laboratory, Wright–Patterson Air Force Base, Ohio 45433
and
Arik F. Johnson†
University of Maryland, College Park, Maryland 20714

DOI: 10.2514/1.36817

Straight tapered geometry approximations to wings with raked tips are presented. Only wings with breaks in the trailing-edge sweep are considered. Comparisons are made with predictions from a vortex-lattice code for a series of uncambered, untwisted wing planforms with raked tips and 10 straight tapered approximations to those planforms. Limited comparisons with experimental data are also shown. Lift-curve slope, aerodynamic center, lateral center of pressure, roll damping and lateral stability are compared for 47 planforms. The most accurate method maintained the area, span, leading-edge sweep, and mean aerodynamic chord of the raked-tip planform, generating a new root and tip chord.

Nomenclature

AR	=	aspect ratio
b	=	wing span
$C_{L\alpha}$	=	lift-curve slope
$C_{l\beta}$	=	rolling moment due to sideslip angle (lateral stability)
C_{lp}	=	rolling moment due to roll date derivative (roll damping)
c_b	=	chord at sweep break
c_r	=	root chord
c_t	=	tip chord
S	=	wing area
x_{ac}	=	longitudinal position of aerodynamic center, measured from apex
y_{cp}	=	lateral position of center of pressure, measured from centerline
α	=	angle of attack
λ	=	taper ratio, c_t/c_r
σ	=	rake angle
Λ	=	sweep angle

Subscripts

$c/2$	=	midchord
eq	=	equivalent planform
le	=	leading-edge
s	=	streamwise
te	=	trailing edge

I. Introduction

WING tips of many configurations are raked for a variety of reasons. Rake is defined in the present paper as having a tip that is nonstreamwise [1]. Many early supersonic missiles (Terrier, Talos, Tartan, Bomarc, etc.) raked the wing tips in an attempt to minimize the lift loss associated with the tip Mach lines. Many missiles and projectiles with deployable tail fins have raked tips. Add-on kits to extend the range of bombs typically include extendable wings that deploy them in a swept state, sometimes leaving a raked tip. Variable-sweep wings on aircraft have tips that are raked as the wing is swept back. The F-15 originally had a streamwise tip that was raked after early flight tests showed higher-than-expected bending loads at transonic speeds. Many modern designs use raked tips to align the edges with other edges on the planform to reduce the radar cross section.

Textbook methods for wing analysis and commonly used design codes such as Missile Datcom [2], MISL3 [3], and AP05 [4] assume that wings are straight tapered (i.e., both root chord and tip chord are streamwise and there are no breaks in the leading- or trailing-edge sweep). Although raked tips can be input into these codes, the accuracy of the algorithms used to generate the equivalent straight tapered planform is not known. Many algorithms for approximating wings with sweep breaks have been published [5–10]. Most maintain the taper ratio of the original planform, which often results in a wing shape with little resemblance to the original planform. The objective of the present work is to assess these algorithms as well as some additional ones to determine which is most suited for planforms with raked tips. The vortex-lattice code HASC02 is used for the bulk of the analysis. Lift-curve slope, aerodynamic center, lateral center of pressure, roll damping, and lateral stability are compared for both the raked-tip planforms and the straight tapered geometry approximations. Limited comparisons are also made with experimental data.

II. Methods Assessed

A generic raked-tip wing is shown in Fig. 1. The nomenclature is from Margolis [1], with the exception that trailing-edge sweep is denoted by Λ_{te}. If the rake angle is zero, the tip chord is streamwise and is given as

$$c_{t,s} = c_r - \frac{b}{2}(\tan\Lambda_{\text{le}} - \tan\Lambda_{\text{te}}) \tag{1}$$

The chord at the sweep break is given as

$$c_b = c_{t,s}\left[1 + \frac{\tan\Lambda_{\text{le}} - \tan\Lambda_{\text{te}}}{\cot\sigma + \tan\Lambda_{\text{te}}}\right] \tag{2}$$

The wing area is given as

Received 24 January 2008; accepted for publication 16 May 2008.

*Senior Aerospace Engineer, Air Vehicles Directorate, 2210 Eighth Street. Associate Fellow AIAA.
†Senior, Department of Aerospace Engineering. Student Member AIAA.

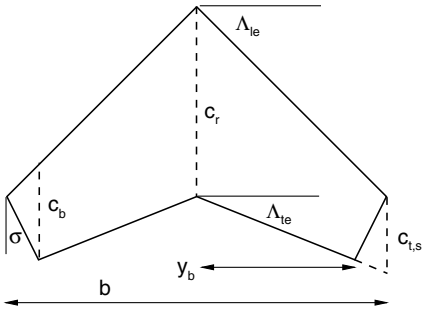

Fig. 1 Raked-wing nomenclature.

$$S = \frac{b}{2}\left[c_r + c_{t,s}\left(1 - \frac{2c_{t,s}}{b\ (\cot\sigma + \tan\Lambda_{\text{te}})}\right)\right] \tag{3}$$

If the spanwise location of the break (y_b) is given instead of the rake angle, the following relations can be used:

$$c_b = c_r - y_b(\tan\Lambda_{\text{le}} - \tan\Lambda_{\text{te}}) \tag{4}$$

$$S = c_r y_b + c_b(b/2) \tag{5}$$

An algorithm that replaces a raked-tip planform with an equivalent straight tapered geometry planform must generate four parameters: aspect ratio, taper ratio, leading-edge sweep, and span. The present paper will assess 10 algorithms for accomplishing this. The first three were studied by Blackmar et al. [5] for wings with breaks in the leading-edge sweep. They maintain area, span, aspect ratio, and taper ratio of the original planform, but differ in how they treat the equivalent sweep.

A. Leading-Edge Sweep Method

This method maintains the leading-edge sweep of the original planform and generates a new root chord. The root chord is calculated using

$$c_{r,\text{eq}} = 2S/b \tag{6}$$

This is one of two methods discussed by Hymer et al. [6] that is used in the AP05 code and is also the method used in Missile Datcom revision 7/07 for lift at supersonic speeds. The Engineering Sciences Data Unit (ESDU) data sheets [7] contain a straight tapered approximation method for wings with a single break in sweep and a separate method for wings with nonstreamwise tips. It is not clear how they categorize raked tips, and so both methods will be assessed in this paper. The leading-edge sweep method is the one recommended for wings with a single break in sweep.

B. C/2 Sweep Method

This method maintains the midchord sweep. Because this varies for a raked wing, Spencer's [8] method is used. Spencer calculates the midchord sweep angle of the equivalent straight tapered planform using the area weighted average of the local midchord sweep angles of the actual planform:

$$\cos\Lambda_{c/2,\text{eq}} = \frac{1}{S}\sum_i S_i \cos\Lambda_{c/2,i} \tag{7}$$

Spencer [8] only used this method to predict lift and did not assume a taper ratio, and so it cannot be used by itself to generate a straight tapered planform. Vukelich et al. [9] recommend use of Spencer's [8] method while retaining the taper ratio of the original planform (as well as span and aspect ratio). The root chord is calculated using Eq. (6), and the leading-edge sweep is calculated from

$$\tan\Lambda_{\text{le,eq}} = \tan\Lambda_{c/2,\text{eq}} + \frac{2}{\text{AR}} \tag{8}$$

This is the method used in Missile Datcom revision 7/07 for lift at subsonic speeds.

C. Trailing-Edge Sweep Method

For straked wings with straight trailing edges, the method recommended by Blackmar et al. [5] maintains the trailing-edge sweep and taper ratio and solves for the equivalent leading-edge sweep. For a raked-tip wing, Blackmar et al. recommend using the area weighted average for the equivalent trailing-edge sweep:

$$\Lambda_{\text{te,eq}} = \frac{1}{S}\sum_i S_i \Lambda_{\text{te},i} \tag{9}$$

$$\tan\Lambda_{\text{le,eq}} = \tan\Lambda_{\text{te,eq}} + \frac{4}{\text{AR}} \tag{10}$$

The root chord is again calculated using Eq. (6). This is the method used in Missile Datcom revision 7/07 for aerodynamic center at all speeds.

The next three methods maintain the leading-edge sweep of the original planform and allow the taper ratio and trailing-edge sweep to vary.

D. Root-Chord Method

This method maintains the root chord and solves for a new tip chord using

$$c_{t,\text{eq}} = \frac{2S}{b} - c_r \tag{11}$$

E. Mean-Chord Method

This method maintains the mean aerodynamic chord instead of the root chord. The mean aerodynamic chord of a raked-tip wing is given by

$$\bar{c} \equiv \frac{2}{S}\int_0^{b/2} c(y)^2 \mathrm{d}y = \frac{2}{3}c_r\left[\frac{1 + c_b/c_r + (c_b/c_r)^2(b/2y_b)}{1 + (c_b/c_r)(b/2y_b)}\right] \tag{12}$$

The taper ratio of the equivalent planform becomes

$$\lambda_{\text{eq}} = -\frac{2S - 3b\bar{c}}{4S - 3b\bar{c}} - \sqrt{\left(\frac{2S - 3b\bar{c}}{4S - 3b\bar{c}}\right)^2 - 1} \tag{13}$$

The root and tip chords of the equivalent planform become

$$c_{r,\text{eq}} = \frac{2S}{b(1 + \lambda_{\text{eq}})} \tag{14}$$

$$c_{t,\text{eq}} = c_{r,\text{eq}}\lambda_{t,\text{eq}} \tag{15}$$

Equation (13) fails to yield a solution if the desired mean aerodynamic chord is greater than $4S/3b$. This is the case for a double-delta wing and is the reason that this algorithm was not studied by Benepe et al. [10] or Blackmar et al. [5] in their studies of cranked-wing planforms. For a wing with a raked tip, the algorithm can only fail for a wing with a concave trailing edge (i.e., if the rake angle minus the trailing-edge sweep angle is greater than 90 deg).

F. Streamwise-Tip Method

This method first adds area aft of the tip to make it streamwise, which makes the equivalent tip chord equal to $c_{t,s}$. The root chord is then reduced to maintain the overall area and span:

$$c_{r,\text{eq}} = \frac{2S}{b} - c_{t,s} \tag{16}$$

This is the method recommended in the ESDU data sheets [7] for wings with tip chords that are not parallel to the vehicle plane of symmetry (i.e., nonstreamwise). This method will yield an inverse

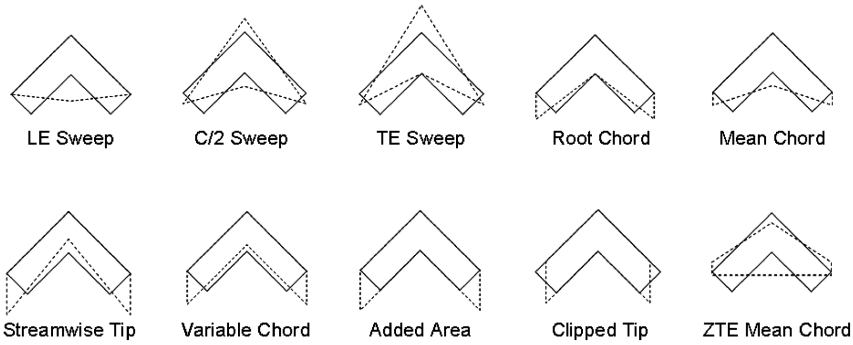

Fig. 2 Straight tapered approximations applied to sample raked-tip planform (LE denotes leading edge, TE denotes trailing edge, and ZTE denotes zero-sweep trailing edge).

taper wing if the leading- and trailing-edge sweeps of the original planform are the same.

The next three methods maintain the leading- and trailing-edge sweeps of the original planform.

G. Variable-Chord Method

In addition to leading- and trailing-edge sweeps, this method maintains wing span and area, which allows both the root chord and tip chord to vary. This is the second of two methods discussed used in AP05 and discussed by Hymer et al. [6]. The equivalent chords are given by

$$c_{r,\text{eq}} = \frac{S}{b} + \frac{b}{4}(\tan\Lambda_{\text{le}} - \tan\Lambda_{\text{te}}) \tag{17}$$

$$c_{t,\text{eq}} = \frac{S}{b} - \frac{b}{4}(\tan\Lambda_{\text{le}} - \tan\Lambda_{\text{te}}) \tag{18}$$

A drawback of this method is that a negative tip chord is possible for a planform with a high aspect ratio.

H. Added-Area Method

This method is similar to the streamwise tip method with the exception that the root chord is unchanged, and so the total area of the wing increases although the span is the same. The wing area increases to

$$S_{\text{eq}} = \frac{b}{2}[c_r + c_{t,s}] \tag{19}$$

Benepe et al. [10] recommend this method for variable-sweep wings with raked tips. Most variable-sweep wings have significant inboard taper, and so the added-area is usually small relative to the basic wing.

I. Clipped-Tip Method

An alternate to the added-area method is to clip the wing tip and attach the clipped area to the trailing edge, creating a streamwise tip while maintaining the overall area. This also maintains root chord but reduces the span. The tip chord becomes

$$c_{t,\text{eq}} = c_{t,s}\left[1 + \left(\frac{2 - c_{t,s}/b - \sqrt{c_{t,s}/c_b}}{1 - c_{t,s}/c_b}\right)\frac{\tan\Lambda_{\text{le}} - \tan\Lambda_{\text{te}}}{\cot\sigma + \tan\Lambda_{\text{te}}}\right] \tag{20}$$

The span is reduced to

$$b_{\text{eq}} = b - \frac{2c_{t,s}}{\cot\sigma + \tan\Lambda_{\text{te}}}\left[\frac{\sqrt{c_{t,s}/c_b} - c_{t,s}/c_b}{1 - c_{t,s}/c_b}\right] \tag{21}$$

The final method fixes the trailing-edge sweep to zero and varies the chord. This is included because the MISL3 code is limited to fins with unswept trailing edges, due to the very large body of data underlying the code, and it is unclear how this limitation affects the approximations. In addition, the method used in Missile Datcom revision 7/07 for the fin lateral center of pressure (at all speeds) is taken from the same database.

J. Zero-Sweep Trailing Edge Mean-Chord Method

This method maintains the mean aerodynamic chord of the original planform and generates a taper ratio of the equivalent planform. The root and tip chords of the equivalent planform are calculated using Eqs. (12–15), and the leading-edge sweep is calculated using

$$\tan\Lambda_{\text{le}} = \frac{4}{\text{AR}}\frac{(1 - \lambda_{\text{eq}})}{(1 + \lambda_{\text{eq}})} \tag{22}$$

Maintaining the leading-edge sweep with an unswept trailing edge was found to be extremely limited in application. It only generates a usable planform if the aspect ratio of the raked planform is less than the aspect ratio of a delta wing with the same leading-edge sweep. If the aspect ratio is higher, a negative taper ratio results from the requirement of an unswept trailing edge.

An application of these algorithms for a sample raked-tip planform is shown in Fig. 2. The leading edge, trailing edge, and rake angles of the planform are 45 deg.

Table 1 summarizes all of the methods and shows what parameters are retained while generating the equivalent planforms.

Table 1 Summary of methods and wing parameters maintained

Method	Ref.	AR	S	b	λ	c_r	$\bar{c}$	Λ_{le}	Λ_{te}
Leading-edge sweep	5–7	✓	✓	✓	✓	——	——	✓	——
Midchord sweep	5, 8, and 9	✓	✓	✓	✓	——	——	——	——
Trailing-edge sweep	5	✓	✓	✓	✓	——	——	——	——
Root chord	——	✓	✓	✓	——	✓	——	✓	——
Mean chord	10	✓	✓	✓	——	——	✓	✓	——
Streamwise tip	7	✓	✓	✓	——	——	——	✓	——
Variable chord	5 and 6	✓	✓	✓	——	——	——	✓	✓
Added area	10	——	——	✓	——	✓	——	✓	✓
Clipped tip	——	——	✓	——	——	✓	——	✓	✓
ZTE mean chord	——	✓	✓	✓	——	——	✓	——	——

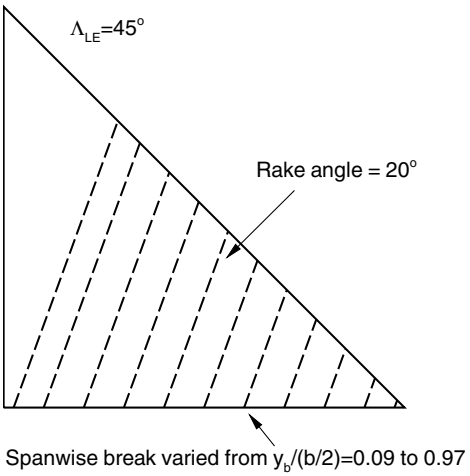

Fig. 3 Wing planform set I.

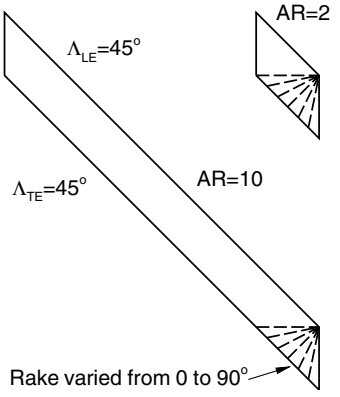

Fig. 4 Wing planform set II.

III. Analytic Results

To assess the approximations, two sets of wing planforms will be examined. The vortex-lattice code HASC02 [11] is used to generate results for the baseline raked-tip planform and each of the 10 approximations. This code was used in an earlier similar study of straked wings [5] and has been shown to provide very good agreement with test data for a variety of configurations. Results will be shown for subsonic ($M = 0.3$) and supersonic ($M = 2.0$) Mach numbers.

The first set of wings has a leading-edge sweep angle of 45 deg, an unswept trailing edge, and a rake angle of 20 deg and varies the spanwise position of the chord break (Fig. 3). The aspect ratio of these planforms varies from 1.13 to 4. These planforms are representative of the wings (or tails) used on the BOMARC, Talos, Terrier, and Bullpup missiles and F-15 and X-45C aircraft.

The second set of wings has parallel leading and trailing edges inboard of the sweep break, with a sweep angle of 45 deg (Fig. 4). The aspect ratio of the wings varies from 2 to over 10 and rake angle varies from 1 to 89 deg for each aspect ratio. These planforms are representative of the wings used on the MGGB, Javelin, and ERGM missiles and the B-2, X-45A, X-47B, and English Electric Lightning aircraft.

Figure 5 shows the error in the lift-curve-slope prediction for the wing set I planform approximations. In all cases, the error is relative to the baseline planform with a raked tip. The results are shown as a function of the spanwise position of the break in the wing chord. As the position of the wing break approaches the semispan ($y_b = b/2$), the wing approaches a delta wing with no tip rake. Each algorithm approaches zero error as the planform approaches pure delta wing, because each algorithm yields the same planform for this limiting case. All of the approximations except the added-area and clipped-tip methods give reasonable results at subsonic speeds, with less than 10% error. The added-area and clipped-tip methods are the only ones that do not maintain the wing aspect ratio. Aspect ratio is probably the single-most-important geometric affecting lift-curve slope, and so this result is not surprising. For the added-area method, the results are based on the increased area of the planform and not the area of the baseline. The Mach 2 trends were the same.

Figure 6 shows the error in the prediction of the longitudinal center of pressure for the wing set I planform approximations. Longitudinal center of pressure is calculated by computing the ratio of the pitching moment and normal force coefficients at a 4 deg angle of attack, with the moment reference center taken at the wing apex. The results are shown as a fraction of the root chord of the baseline raked-tip planform. Again, only the subsonic results are shown, and the supersonic results were very similar. Like the lift results, all of the approximations approach zero error as the planform approaches a pure delta wing. For the longitudinal center-of-pressure prediction, the relative alignment of the apex of the approximate planform relative to baseline raked-tip planform is critical. Two alignments were studied. These were 1) maintaining the apex at the same position (as shown in Fig. 1) and 2) shifting the apex so that the area centroid of the panels would coincide (as shown in Fig. 2). Results shown for the root-chord, streamwise-tip, added-area, and clipped-tip methods are based on apex alignment, and all other results are based on centroid alignment. Inspection of Fig. 6 shows that the methods that maintain leading-edge sweep but allow chord to vary (root chord, mean chord, and streamwise tip) give excellent results for all planforms. The leading-edge sweep, added-area, and variable-chord methods give fair results, whereas all of the other methods give very poor results. As the position of the wing break approaches the root ($y_b = 0$), the added-area method almost doubles the total wing

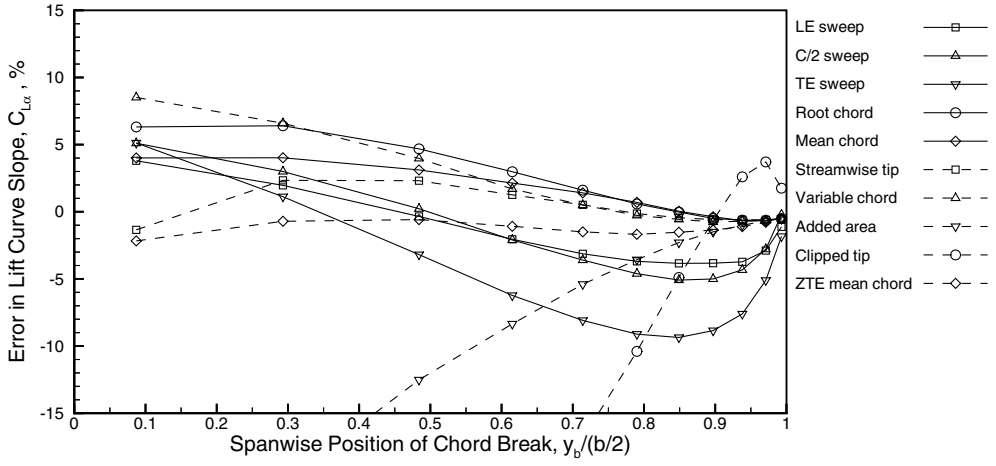

Fig. 5 Lift prediction accuracy for wing set I, Mach = 0.3.

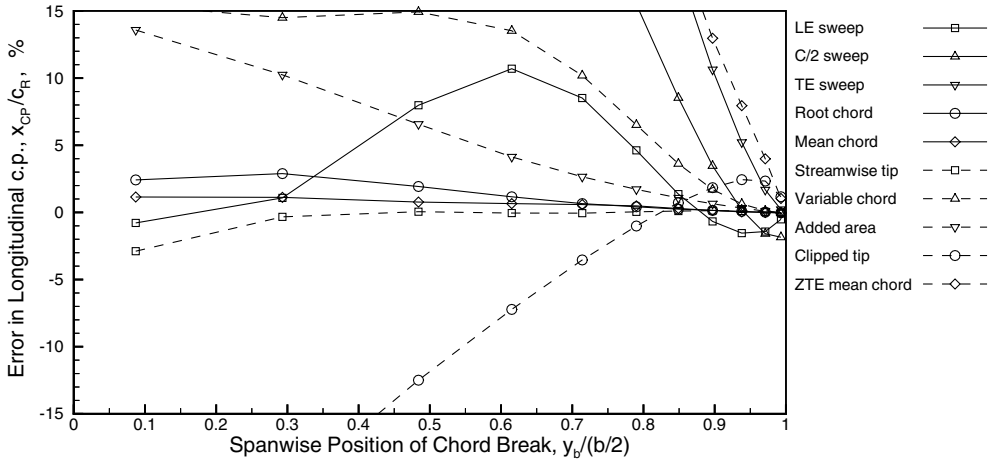

Fig. 6 Longitudinal center-of-pressure prediction accuracy for wing set I, Mach = 0.3.

area when compared with the baseline. The fact that this is one of the better methods for center-of-pressure prediction indicates the importance of the distribution of area on the planform.

The effect of adding the requirement of an unswept trailing edge can be seen on this and all subsequent figures by comparing the solid and dashed lines with the diamond symbol. The solid line represents the basic mean-chord approximation (with leading-edge sweep maintained), and the dashed line is the mean-chord approximation with zero trailing-edge sweep. Even after the planform centroid is aligned, the unswept trailing-edge approximation is significantly worse for longitudinal center of pressure.

Figure 7 shows the error in the lateral center-of-pressure prediction for the wing set I planform approximations at Mach 2. The mean-chord method provides exceptional results, with maximum errors of less than 2%. None of the other methods were consistently within 5% error. The subsonic results showed much better accuracy, with almost all methods within 5% of the wing semispan.

Figure 8 shows the error in the prediction of roll damping for the wing set I planform approximations at Mach 0.3. Like the lift results, all but two of the methods are within about 10% for most of the cases, with the added-area and clipped-tip methods providing the worst predictions. These are the only methods that do not maintain the wing aspect ratio. Of the remaining methods, the best are those that do not maintain zero taper ratio. Roll damping is known to be highly dependent on taper ratio. The Mach 2 results were very similar.

Figure 9 shows the error in the prediction of lateral stability damping for the wing set I planform approximations at Mach 0.3. The parameter shown is the lateral stability derivative $C_{l\beta}$ divided by the wing lift coefficient, because the wing contribution to lateral stability is proportional to lift [10]. The wings were evaluated with no dihedral, and so the effect shown is primarily a sweep effect. The results show that the majority of the approximations give very poor predictions, with only four giving errors of less than 50% across the range of planforms. The leading-edge sweep and mean-chord methods show the best results for this wing set. The same trends were found in the Mach 2 results.

Figure 10 shows the error in the prediction of lift-curve slope for the wing set II planform approximations at Mach 2. The results are shown as a function of the aspect ratio of the baseline raked-tip planform. This figure shows five sets of planforms, corresponding to aspect ratios of 2, 4, 6, 8, and 10 of the baseline planform. As the rake angle increases, the aspect ratio increases slightly due to the decrease in area (see Fig. 4). Almost without exception, the errors decrease as the aspect ratio of the baseline planform increases. In addition, the errors tend to decrease as the rake angle decreases. This is because the lowest rake angle considered for each set (1 deg) essentially corresponds to an unraked planform. As the rake angle approaches zero, the errors from the leading-edge and trailing-edge sweep methods do not approach zero, because the planforms from these methods are not asymptotic to the actual planform as rake approaches zero.

Figure 11 shows the error in the prediction of longitudinal center of pressure for the wing set II planform approximations at Mach 0.3. Like the lift results, the errors decrease as the aspect ratio of the baseline planform increases. The methods that allow taper to vary also improve as rake angle decreases, as expected. The root-chord method is clearly the best, with the variable-chord and mean-chord methods also giving good results. For the supersonic cases, these three methods were also the best, with the clipped-tip method also giving reasonable results.

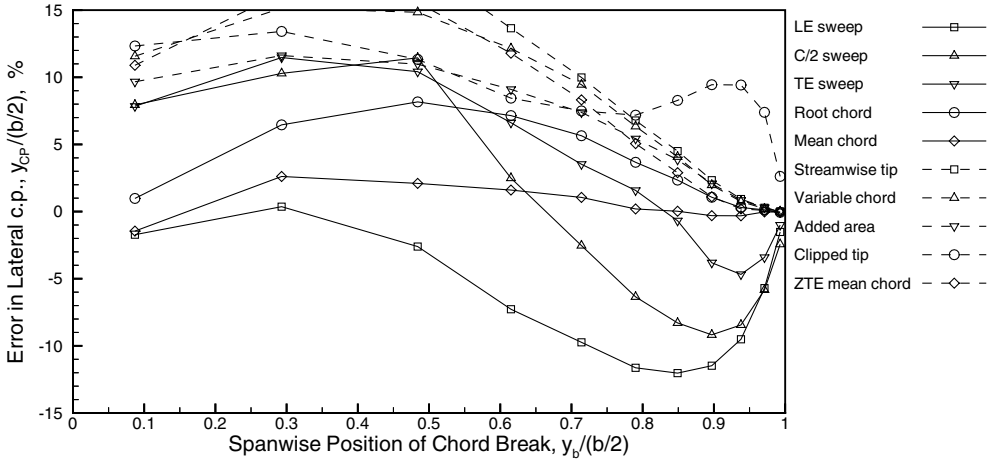

Fig. 7 Lateral center-of-pressure prediction accuracy for wing set I, Mach = 2.

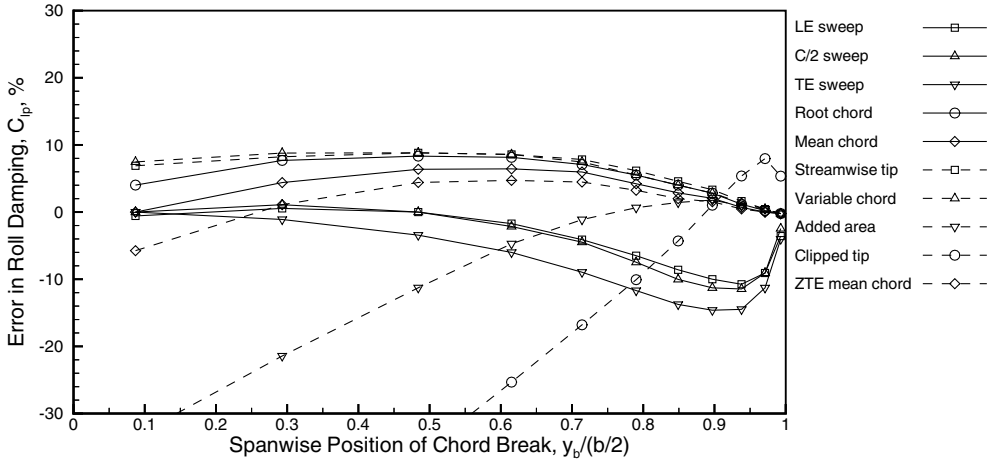

Fig. 8 Roll damping prediction accuracy for wing set I, Mach = 0.3.

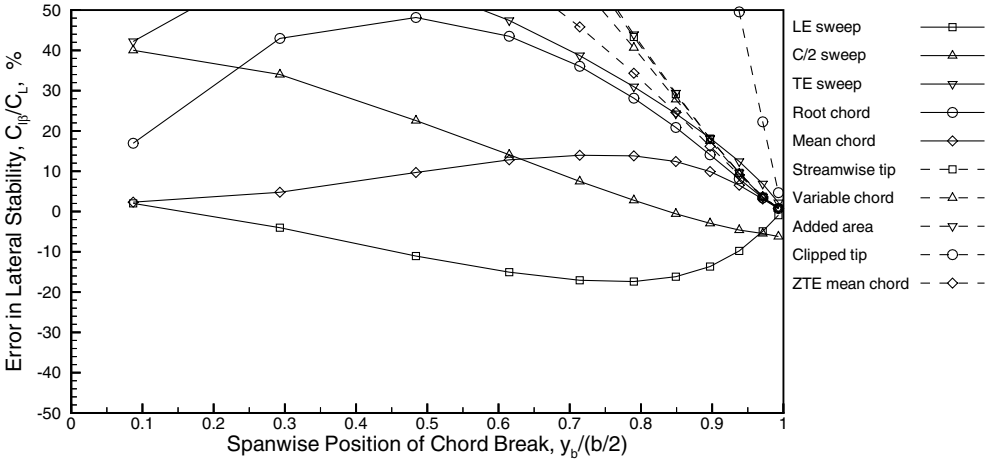

Fig. 9 Lateral stability prediction accuracy for wing set I, Mach = 0.3.

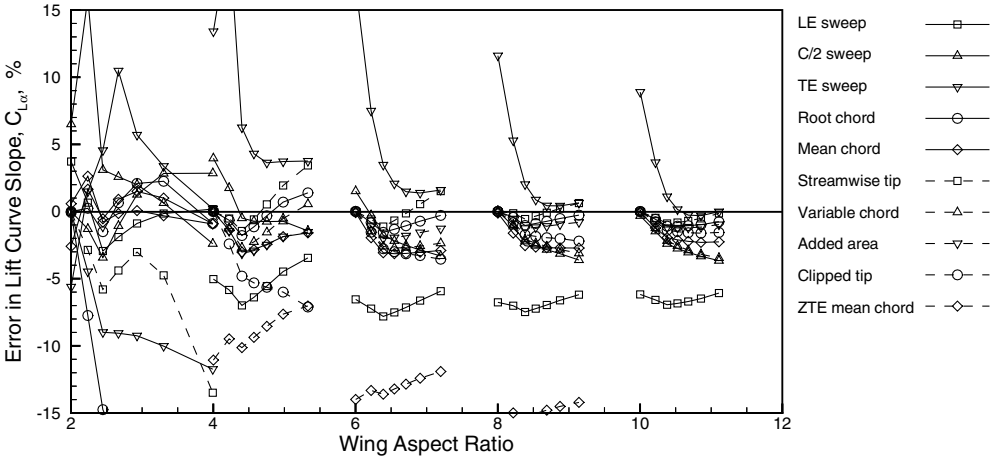

Fig. 10 Lift prediction accuracy for wing set II, Mach = 2.

Figure 12 shows the error in the prediction of lateral center of pressure for the wing set II planform approximations at Mach 0.3. Once again, the errors decrease as the aspect ratio of the baseline planform increases and also decrease as the rake angle decreases. The root-chord and mean-chord methods are the best, with the root-chord method superior at the higher aspect ratios and with the mean-chord method superior for lower aspect ratios. The Mach 2 results were very similar.

Figure 13 shows the error in the prediction of roll damping for the wing set II planform approximations at Mach 2. Like the lateral center-of-pressure result, the methods that maintain zero taper are poor. Only the mean-chord method gives consistently good results. The Mach 2 results were similar.

Figure 14 shows the error in the prediction of lateral stability for the wing set II planform approximations for Mach 2. The mean-chord method is clearly superior to the entire range of aspect ratios.

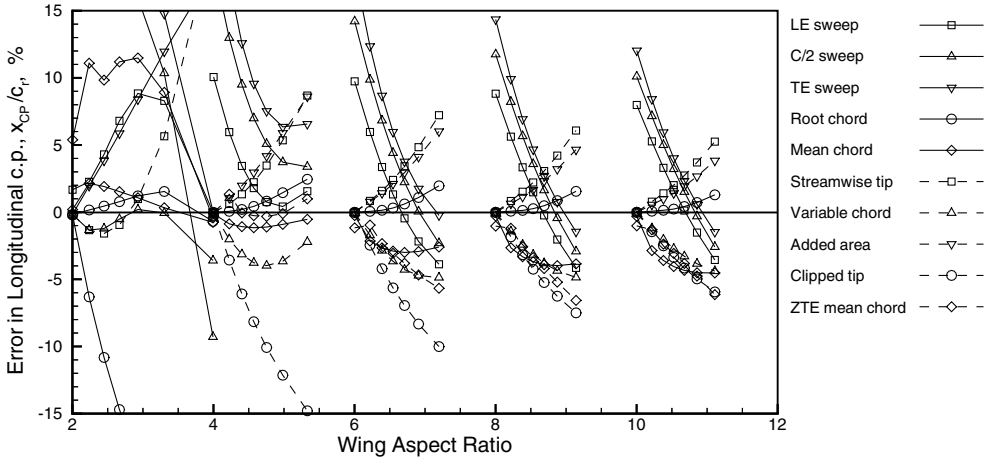

Fig. 11 Longitudinal center-of-pressure prediction accuracy for wing set II, Mach = 0.3.

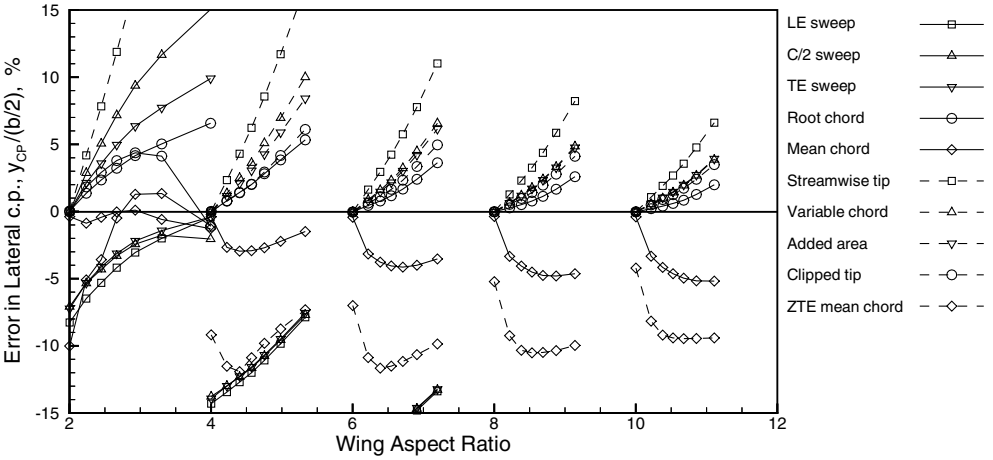

Fig. 12 Lateral center-of-pressure prediction accuracy for wing set II, Mach = 0.3.

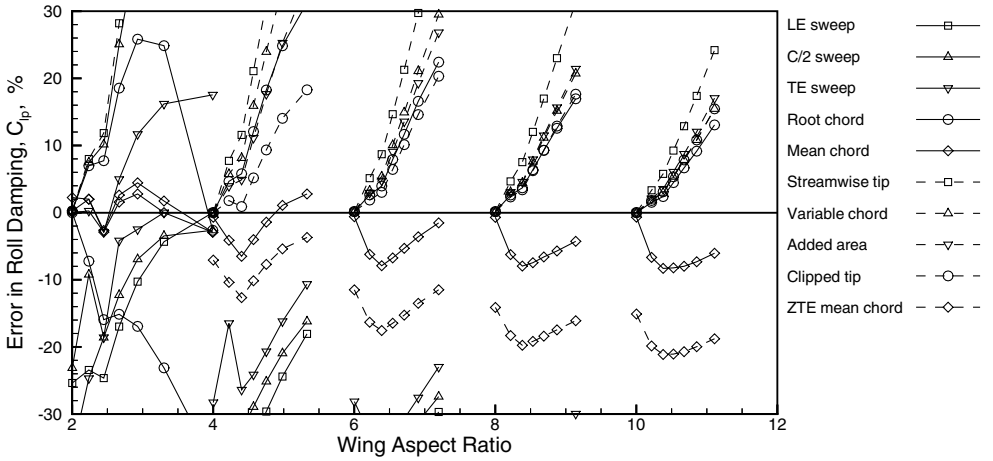

Fig. 13 Roll damping prediction accuracy for wing set II, Mach = 2.

Table 2 shows how well each method did for each parameter for both wing sets. Instead of average error, the maximum error is shown. The reason for this is to help determine not what the best method is for each case, but which method (or methods) is most robust method when all cases are considered. The errors shown were determined from previous studies of the accuracy of handbook-type methods and from engineering judgment. A single or double check mark indicates that the method was as accurate as the value shown for every wing planform studied at both subsonic and supersonic speeds. The mean-chord method is the only one that was within the established accuracy for each parameter for each wing set. It was not the most accurate for each case, but was the most consistent performer. In terms of average accuracy, the streamwise-tip method was the best for lift for wing set I, and the root-chord method was the best for lift and both centers of pressure for wing set II. The mean-chord method was the best for all of the other wing sets and parameters.

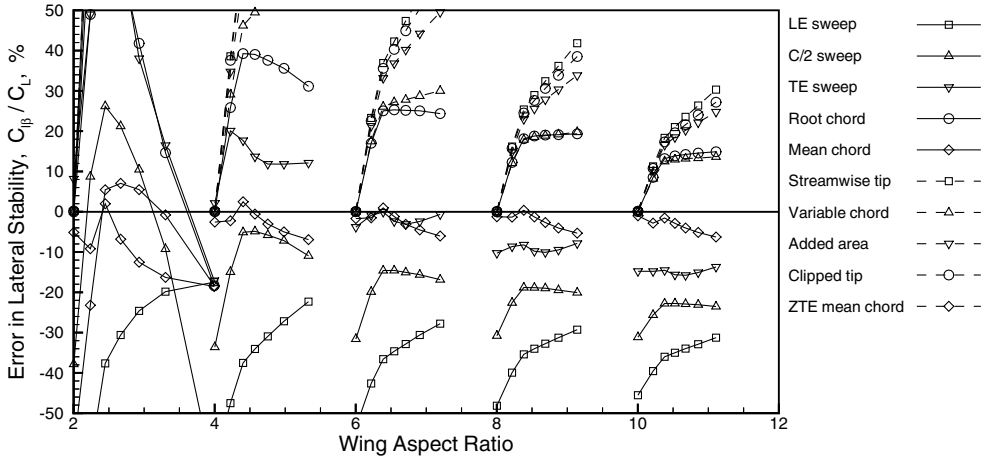

Fig. 14 Lateral stability prediction accuracy for wing set II, Mach = 2.

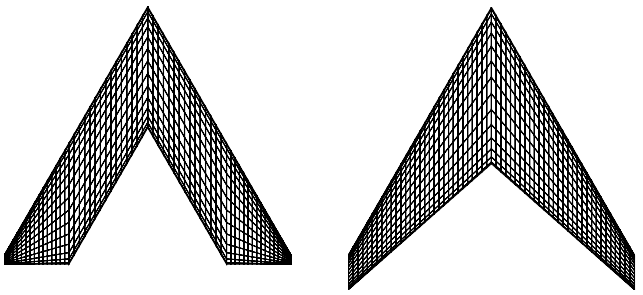

Fig. 15 Mansell wing geometry and mean-chord approximation.

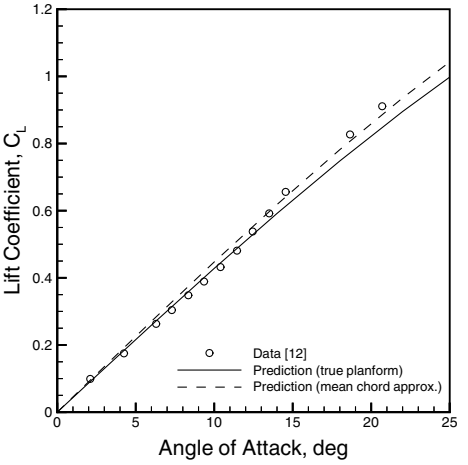

Fig. 16 Mansell wing lift comparison.

IV. Comparisons with Experimental Data

Although numerous reports exist with experimental data of wings with raked tips, most contain plotted data only and many are not in the open literature. Comparisons with test data will be shown for two configurations for which numerical data were available. Extracting longitudinal center of pressure from published plots of pitching moment often results in uncertainty equal to or larger than the differences between the analytic results shown in the previous section.

Mansell [12] gave test data for an isolated wing with leading- and trailing-edge sweeps of 60 and 90 deg of rake. The wing is untwisted with a symmetric airfoil section. The planform is extremely similar to that used on the English Electric Lightning fighter. The HASC02 representations of the Mansell wing and the mean-chord approximation are shown in Fig. 15. Figures 16 and 17 compare the measured lift and center-of-pressure data with the HASC02 results. Both the true planform representation and mean-chord approximation give excellent agreement with the lift and center-of-pressure data. The vertical scale of the c.p. plot is magnified, showing a c.p. just slightly aft of the trailing edge of the root chord. The separation on the outboard panel that results in a forward c.p. shift at higher angles of attack is not predicted with either model.

Reed [13] gave test data for a chevron wing with 45 deg leading-edge sweep at subsonic speed. The HASC02 representations of the chevron wing and the mean-chord approximation are shown in Fig. 18. The wing span is 2.15 times the root chord, which makes it very close to the aspect ratio 2 wing from wing set II. The wing is untwisted with a symmetric airfoil section. Figures 19 and 20 compare the measured lift and center-of-pressure data with the predictions. Excellent agreement with the lift data is evident for both

Table 2 Maximum error of methods studied

Method	$C_{L\alpha}$		x_{cp}/c_r		$y_{cp}/(b/2)$		C_{lp}		$C_{l\beta}/C_L$	
Maximum error	✓✓	<10%	✓✓	<5%	✓✓	<5%	✓✓	<10%	✓✓	<25%
	✓	<20%	✓	<10%	✓	<10%	✓	<20%	✓	<50%
Wing set	I	II	I	II	I	II	I	II	I	II
Leading-edge sweep	✓✓	✓	✓	✓	—	—	✓	—	✓	—
Midchord sweep	✓	✓	—	—	—	—	—	—	✓	✓
Trailing-edge sweep	✓	—	—	—	—	—	✓	—	—	—
Root chord	✓	✓✓	✓	✓✓	✓	—	✓	—	—	—
Mean chord	✓✓	✓✓	✓✓	✓	✓✓	✓	✓	✓✓	✓✓	✓✓
Streamwise tip	✓✓	—	✓	—	—	—	✓	—	—	—
Variable chord	✓	✓✓	—	✓	—	—	✓	—	—	—
Added area	—	—	—	—	—	—	—	—	—	—
Clipped tip	—	—	—	—	—	—	—	—	—	—
ZTE mean chord	✓✓	—	—	—	—	—	✓	—	—	—

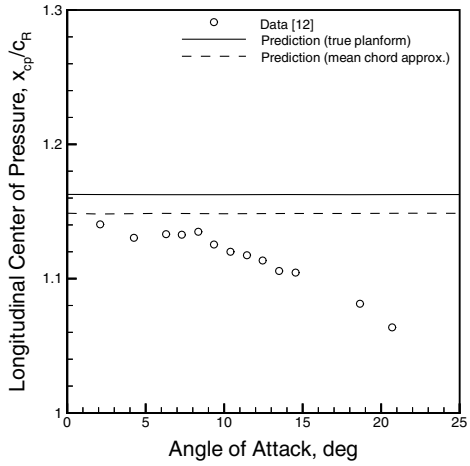

Fig. 17 Mansell wing center-of-pressure comparison.

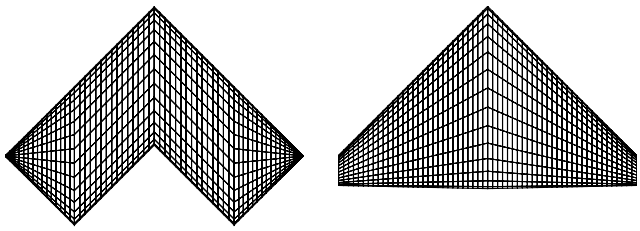

Fig. 18 Chevron wing geometry and mean-chord approximation.

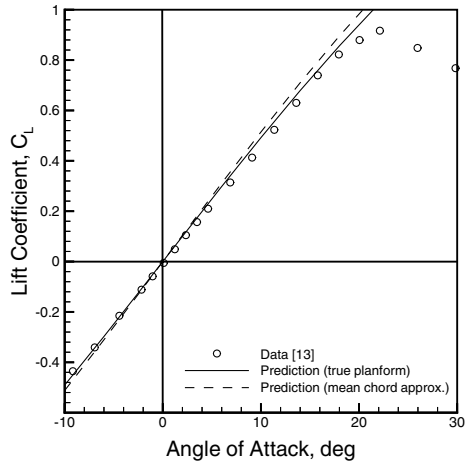

Fig. 19 Chevron wing lift comparison.

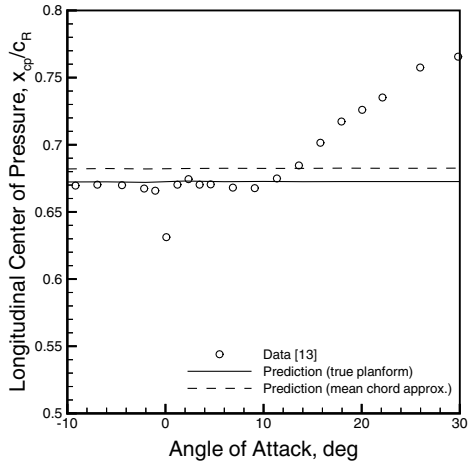

Fig. 20 Chevron wing center-of-pressure comparison.

the true planform representation and mean-chord approximation. The true planform representation is in perfect agreement with the center-of-pressure test data at low angles of attack, whereas the mean-chord approximation gives a result that is less than 2% of the root chord aft.

V. Conclusions

A study of straight tapered geometry approximations to wings with raked tips has been presented. Only wings with breaks in the trailing-edge sweep were considered. Ten approximation algorithms were assessed. Three of these had been studied earlier for wings with breaks in the leading-edge sweep. Four had been previously published, but without substantiation, and the remaining three were newly developed for this study. To assess the relative accuracy of the approximations, comparisons were made with predictions from a vortex-lattice code for a series of uncambered, untwisted wing planforms. Lift-curve slope, aerodynamic center, lateral center of pressure, roll damping, and lateral stability were compared for 47 different planforms. The preferred method maintained the area, span, leading-edge sweep, and mean aerodynamic chord of the baseline planform, generating a new root and tip chord. It also compared very well with limited experimental data.

References

[1] Margolis, K., "Theoretical Lift and Damping on Roll of Thin Sweptback Tapered Wings with Raked-In and Cross-Stream Wing Tips at Supersonic Speeds," NACA TN 2048, Mar. 1950.

[2] Blake, W. B., "Missile Datcom User's Manual—5/97 Fortran 90 Revision," U.S. Air Force Research Lab., Rept. VA-WP-TR-1998-3009, Wright–Patterson AFB, OH, Feb. 1998.

[3] Lesieutre, D. J., Love, J. F., Dillenius, M. F. E., and Blair, A. B., "Recent Applications and Improvements to the Engineering Level Aerodynamic Prediction Software MISL3," AIAA Aerospace Sciences Conference, AIAA Paper 2002-0275, Jan. 2002.

[4] Moore, F. G., and Hymer, T. C., "2005 Version of the Aeroprediction Code (AP05)," *Journal of Spacecraft and Rockets*, Vol. 42, No. 2, Mar.–Apr. 2005, pp. 240–256.

[5] Blackmar, S. C., Miller, M. S., and Blake, W. B., "Approximate Methods for Center of Pressure Prediction of Multi-Segment Wings," AIAA Applied Aerodynamics Conference, AIAA Paper 2003-3934, Orlando FL, June 2003.

[6] Hymer, T. C., Moore, F. G., and Downs, C., "User's Guide for an Interactive Personal Computer Interface for the 1998 Aeroprediction Code (AP98)," Naval Surface Warfare Center, Dahlgren Div., TR-98/7, Dahlgren, VA, June 1998.

[7] "Geometrical Properties of Cranked and Straight Tapered Planforms," Engineering Sciences Data Unit, Data Sheet 76003, Jan. 1976, Amendment A, London, Oct. 1981.

[8] Spencer, B., Jr., "A Simplified Method for Estimating Lift Curve Slope at Low Angles of Attack for Irregular Planform Wings," NASA TM X-525, May 1961.

[9] Vukelich, S. R., Stoy, S. L., Burns, K. A., Castillo, J. A., and Moore, M. E., "Missile Datcom Volume 1: Final Report," U.S. Air Force, Wright Aeronautical Labs. TR-86-3091, Wright–Patterson AFB, OH, Dec. 1988.

[10] Benepe, D. B., Kouri, B. G., and Webb, J. B., "Aerodynamic Characteristics of Non-Straight Taper Wings," U.S. Air Force, Flight Dynamics Lab. TR-66-73, Wright–Patterson AFB, OH, Oct. 1966.

[11] Albright, A. E., Dixon, C. J., and Hegedus, M. C., "Modification and Validation of Conceptual Design Aerodynamic Prediction Method HASC95 with VTXCHN," NASA CR 4712, Mar. 1996.

[12] Mansell, C. J., "Low Speed Wind Tunnel Test on Two Thin Cranked Wings with 60-deg Sweepback Inboard," Aeronautical Research Council Reports and Memoranda No. 2995, London, 1957.

[13] Reed, S. A., "Experimental Aerodynamic Development of Advanced Unmanned Combat Aerial Vehicle Configurations," U.S. Air Force Research Lab., Rept. VA-WP-TR-1998-3076, Wright–Patterson AFB, OH, Oct. 1998.

M. Miller
Associate Editor